Structural Engineering and Mechanics, Vol. 11, No. 1 (2001) 35-48
DOI: http://dx.doi.org/10.12989/sem.2001.11.1.035

Stability analysis of steel cable-stayed bridges

Chia-Chih Tang†, Hung-Shan Shu† and Yang-Cheng Wang‡

Department of Civil Engineering, Chinese Military Academy, Taiwan,
1 Hwang-Poo Road, Feng-Shan, 83000, Taiwan, ROC

Abstract. The objective of this study is to investigate the stability behavior of steel cable-stayed bridges by comparing the buckling loads obtained by means of finite element methods with eigen-solver. In recent days, cable-stayed bridges dramatically attract engineers' attention due to their structural characteristics and aesthetics. They require a number of design parameters and present a high degree of static indetermination, especially for long span bridges. Cable-stayed bridges exhibit several nonlinear behaviors concurrently under normal design loads due to the individual nonlinearity of substructures such as the pylons, stay cables, and bridge deck, and their interactions. The geometric nonlinearities arise mainly from large displacements of cables. Strong axial and lateral forces acting on the bridge deck and pylons cause structural nonlinear behaviors. The interaction is among the substructures. In this paper, a typical three-span steel cable-stayed bridge with a variety of design parameters has been investigated. The numerical results indicate that the design parameters such as the ratio of L_1/L and I_p/I_b are important for the structural behavior, where L_1 is the main span length, L is the total span length of the bridge, I_p is the moment of inertia of the pylon, and I_b is the moment of inertia of the bridge deck. When the ratio I_p/I_b increases, the critical load decreases due to the lack of interaction among substructures. Cable arrangements and the height of pylon are another important factors for this type of bridge in buckling analysis. According to numerical results, the bridges supported by a pylon with harp-type cable arrangement have higher critical loads than the bridges supported by a pylon with fan-type cable arrangement. On contrary, the shape of the pylon does not significantly affect the critical load of this type of bridge. All numerical results have been non-dimensionalized and presented in both tabular and graphical forms.

Key words: stability analysis; cable-stayed bridges; steel and bridge.

Introduction

Since the eighteenth century cable-stayed bridges have been known but they have been widely built only in the last few decades (ASCE 1992, Xanthakos 1994). The increasing popularity of contemporary cable-stayed bridges among bridge engineers can be attributed to (1) the appealing aesthetics; (2) the full and efficient utilization of structural materials; (3) the increased stiffness over suspension bridges; (4) the efficient and fast mode of construction; and (5) the relatively small size of the bridge elements (Ren and Obata 1999). The first modern cable-stayed bridge was designed and built in Sweden, completed in 1955 (Xanthakos 1994). The bridge has spans of 74 m, 183 m and 74 m. According to recent experience, cable-stayed bridges are suited for clear spans in the range of 120 m to 600 m (Ito 1998), and have girders made of steel or prestressed concrete. Ren

† Lecturer
‡ Professor

and Obata (1999) even state that cable-stayed bridges are now entering a new era, reaching central span lengths ranging from 400 to 1,000 m or longer. They also point out that the rapid progress is largely due to (1) the development of box-girders with orthotropic plate decks; (2) the manufacturing techniques of high-strength wires that can be used for stayed cables; (3) the use of electronic computers in structural analysis and design; and (4) the advances in prestressed concrete structures. As the span length increases, the stability characteristics of cable-stayed bridges become more important and more complex.

A favorable aspect of the construction of cable-stayed bridges is that this type of structure can be erected without falsework in the main span, and this represents a considerable advantage for bridges over deep canyons or waterways. Many cable-stayed bridges have been built over famous waterways and rivers in Europe (Capra *et al.* 1998), Canada, South America, Asia, and the United States (Modjeski and Masters 1983, Committee on General Structures Subcommittee on Bridge Aesthetics, ASCE 1991). The ASCE Committee on Long-Span Steel Bridges (1988) provides an extensive bibliography and data on cable-stayed bridges.

Since cables instead of interval piers support the deck in cable-stayed bridges, they are much more flexible than conventional continuous bridges, especially for long span. A long span cable-stayed bridge exhibits nonlinear characteristics under normal design load. It is well known that these long span cable-supported structures are composed of complex structural components with high geometric nonlinearities (Ren 1999). Due to the characteristics of the structural supporting conditions (Wang *et al*. 1993), bridge decks and pylons are subjected to strong axial forces arising from cable reactions. The axial forces acting on the bridge deck and pylons will cause geometrically nonlinear behavior. In addition to the axial forces, some of the most important factors on stability analysis of cable-stayed bridges are the cable nonlinearity due to its own sag, the interaction between the cables and the bridge deck, and the interaction between the cables and the pylons.

With high compressive forces in both girders and pylons, the stability of cable-stayed bridges has been a concern for bridge engineers (Xi and Kuang 1999). For stability consideration, a number of characteristics of cable-stayed bridges must be included such as span length (Simoes *et al.* 1994), the use of concrete (Cluley *et al.* 1996), steel or composite superstructure (Adeli *et al.* 1995), vehicular or pedestrian bridges (Yang *et al.* 1998, Gardner-Morse 1993), the structural behavior of cables (Leu *et al.* 1996, Walton 1996, and Wang *et al*. 1997, Wang 1999a and 1999c), dimensions of pylons and bridge deck, and erection or fabrication methods (Freeman 1994, Oh *et al.* 1998). Xanthakos (1994) stated that the design of a cable-stayed bridge has mainly to satisfy the serviceability and safety requirements in terms of limited girder and tower deflections and limited cable, girder, and tower stress. Because of the nonseparable nature of the parameters, it may be difficult to isolate any single parameter and study its effect on the behavior of the bridge. Agrawal (1997, 1998) also stated that a parametric study is necessary because it gives the idea of the effect of the various parameters on forces and displacements in cable-stayed bridges. Although the various parameters are nonseparable, at the same time, it is not possible to incorporate the effect of all parameters at one time.

With the use of digital technology, numerical methods, and high strength materials, the span length of cable-stayed bridges can be increased. The bridge deck then becomes more flexible compared to those of conventional continuous bridges. Researchers became interested in the behavior of cable-stayed bridges as a result of their efficient use of materials and their pleasant aesthetics (Committee on General Structures Subcommittee on Bridge Aesthetics, ASCE 1991). Some of the researchers analyzed the behavior of cable-stayed bridges by using finite element

methods. Many types of modeling have been reported (Wilson 1991, Hua and Wang 1996, and Wang *et al*. 1998). Although two-dimensional finite element models have been widely studied, only the flexural mode has been considered. In order to estimate the importance of the lateral and torsional modes as well as their coupled modes for stability analysis, three-dimensional analysis should be called upon, especially for long span bridges.

2. Geometry and loading

With a variety of design parameters, a typical three-span steel cable-stayed bridge supported by different cable arrangements has been investigated in this paper. The bridge is subjected to three different types of load condition. The geometry of the bridge and its loading conditions are described in the following sections.

2.1. Geometry

Cable-stayed bridges consist of three primary parts: the pylons, deck, and stayed cables; their four basic longitudinal cable configurations are: harp-type, fan-type, radiating-type, and star-type (Agrawal 1997 and 1998). The cable-stayed bridges to be analyzed herein consist of different cable arrangements, various shapes of pylon, and a variety of designed parameters. The harp-type and fan-type cable configurations are only considered in this paper. In the harp-type, the cables are parallel and spaced along the girder and the pylon as shown in Fig. 1(a). The radiating-type is a converging system where the cables intersect at a common point at the top of the pylon. In the star-type cable arrangement, the cables are spaced along the pylon and converge at a common point on

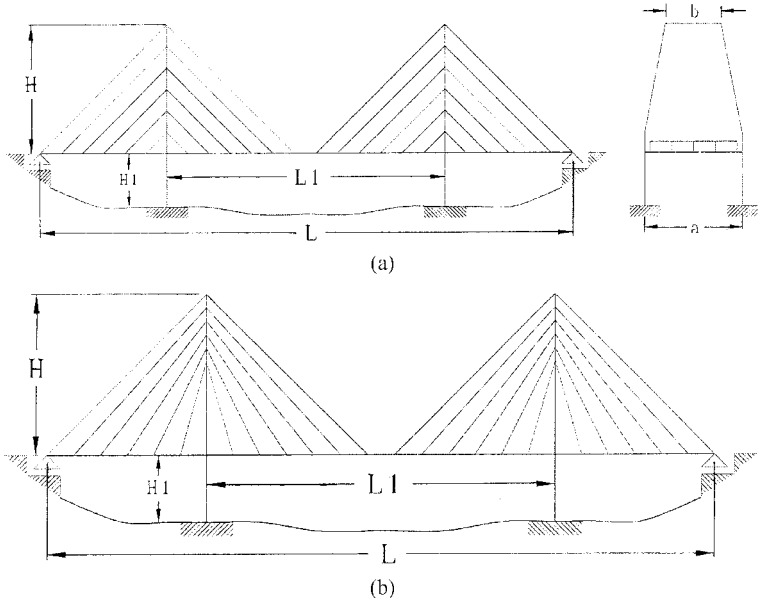

Fig. 1 (a) Geometry of harp-type cable-stayed bridge, (b) Geometry of fan-type cable-stayed bridge

the girder (Agrawal 1997). The fan-type cable arrangement combines the harp-type and radiating-types shown as in Fig. 1(b). In Figs. 1(a) and 1(b), 24 stay cables each support the bridge in a fan-type or harp-type cable arrangement.

In this paper, the shapes of pylon vary from A-type to H-type depending on the designed parameter b/a ranging from 0.0 to 1.0 in which a is the length of the lower strut that is fixed equal to 20 m, and b is a design parameter representing the distance between the tops of the columns. In another words, if b/a is zero, the pylon is A-type; if b/a is 1.0, the pylon is H-type.

The design parameters depend on the geometric properties of the pylons and the bridge deck that is a composite steel girder. The total span length L is 460 m and the height of the pylon from pier bottom to bridge deck H_1 is 30 m; L and H_1 remain constant. The main-span length L_1 and the height of the pylon above the level of the bridge deck H are considered as design parameters proportional to the total span length. For a constant cross section of the bridge deck, the moment of inertia of the bridge deck, I_b is constant. In order to investigate interaction among the substructures, the moment of inertia of the pylon I_p is considered a design variable. For parametric study, Table 1 represents the designed parameters L_1/L, I_p/I_b, H/L, and b/a.

2.2. Loading

Three types of loading condition are considered: a full lane load, a half lane load, and a diagonal half lane load. In the full lane loading, the bridge deck is covered by a uniform lane load. In the half lane loading, one half width of the bridge deck is covered by a uniform lane load symmetrically along the longitudinal direction. In the diagonal half lane loading is one half width of the bridge deck is covered by a uniform lane load symmetrically about the central point of the deck.

3. Finite element model

Bathe (1982) indicates that during the past two decades, the finite element method of analysis has rapidly become a very popular technique for the computer solution of complex problem in engineering. At present, the finite element method represents the most general tool for analysis and is used in practically all fields of engineering. In this paper, the finite element method with an eigen-solver has been used to investigate the stability behavior of steel cable-stayed bridges.

The bridge deck is a three-cell steel box girder with the width of 18 m and the deep of 2 m. In another words, the box girder has two internal and two outside webs, respectively. The thickness of the web is 0.15 m, and the thickness of the slab as well as the bottom of the box girder is 0.25 m.

Three types of element, shell, beam, and tension-only spar, have been used to model the bridge. First, there are 1840 single-layer quad-shell elements to model the box steel girder. There are 1380

Table 1 The parameters of the bridge geometry

Parameter	Ratios				
L_1/L	0.40	0.50	0.60	0.70	0.80
I_p/I_b	0.10	1.00	2.50	5.00	10.0
H/L	0.10	0.20	0.30	0.40	0.50
b/a	0.00	0.25	0.50	0.75	1.00

elements to model the slab and the bottom of the box girder, and the size of each element remains the same as 3 m by 2 m. There are 460 elements to model the four webs of the box girder, and the size of each element also remains the same as 4 m by 2 m.

Then, 20 three-dimensional beam elements model each pylon; 3 three-dimensional beam elements model each strut that connects two towers of the pylon. Each node of shell and beam element incorporates six degrees of freedom, i.e. translation in x, y and z directions as well as rotation about the x, y and z axes. Last, each tension-only spar element models a stay cable; each node of the element consists of only three translational degrees of freedom. For the cable element, the cable stiffness will be taken as zero if it is subjected to compressive forces.

In order to precisely model the structure, idealizations are made as follows.

1. All parts are originally straight; i.e. no geometric imperfections are taken into account in this paper.
2. The material behavior is linearly elastic and the moduli of elasticity E in tension and compression are equal.
3. For steel shell element, the modulus of elasticity E is 200 Gpa; Poisson's ratio ν is 0.3; and the mass density is 7860 Kg/m^3.
4. For concrete pylon and strut, the modulus of elasticity E is 30 Gpa; Poisson's ratio ν is 0.25; and the mass density is 2320 Kg/m^3.

4. Numerical results

The critical loads and their corresponding buckling mode shapes are found by using eigen-buckling analysis according to the finite element model and the solution procedure (Ermopoulos *et al.* 1992 and Vlahinos *et al*. 1993). A wide range of the design parameters of the bridge is studied in this paper as listed in Table 1.

Table 2 represents the non-dimensional critical loads of the bridge supported by a H-type pylon with harp-type cable arrangement, and with designed parameters L_1/L, H/L, and I_p/I_b, under full lane load condition. The non-dimensional critical load has been taken as $\overline{Q}_{cr}=Q_{cr}L^3/EI_b$ where Q_{cr} is the numerical result obtained by eigen-buckling analysis of the bridge; L is the total span length; and, EI_b is the rigidity of the bridge deck. Table 2 represents the tabular form of the numerical results of the first 6 critical load, and Fig. 2(a) represents their corresponding mode shapes. The first 4 critical loads are identical. The corresponding mode shapes of the first two modes are symmetric because the bridge is symmetric. Even though the first 4 modes have the same critical load, the corresponding mode shapes of the third and fourth buckling mode are different from those of the first and the second modes. The fourth mode represents more significant torsional behavior than that of the third mode although they have the same critical load. The critical loads of the fifth and the sixth mode are identical, but their corresponding mode shapes are anti-symmetric. In Table 2, the results implicate that if L_1/L or H/L decreases, the critical load increases due to the lack of the interaction between the pylons and the bridge deck.

Table 3 lists the non-dimensional critical loads of the bridge supported by H-type pylon with fan-type cable arrangement, and with the same design parameters as those of Table 2. Fig. 2(b) shows their first 6 corresponding mode shapes. Most of the structural characteristics of these two types of bridge are similar, but the fan-type bridges always have lower critical loads than those of the harp-type bridges. The different cable arrangements have different angles between the bridge deck and

Table 2 Non-dimensional critical loads of harp-type bridge subjected to full lane load with H-type pylon

I_p/I_b	H/L	L_1/L																	
		0.4						0.6						0.8					
		1st Mode	2nd Mode	3rd Mode	4th Mode	5th Mode	6th Mode	1st Mode	2nd Mode	3rd Mode	4th Mode	5th Mode	6th Mode	1st Mode	2nd Mode	3rd Mode	4th Mode	5th Mode	6th Mode
0.10	0.10	0.0576	0.0576	0.0576	0.0576	0.0683	0.0683	0.0356	0.0356	0.0357	0.0356	0.0445	0.0445	0.0172	0.0172	0.0172	0.0172	0.0179	0.0179
	0.30	0.0576	0.0576	0.0576	0.0576	0.0684	0.0684	0.0356	0.0356	0.0357	0.0357	0.0445	0.0445	0.0172	0.0172	0.0172	0.0172	0.0179	0.0179
	0.50	0.0577	0.0577	0.0577	0.0577	0.0684	0.0684	0.0357	0.0357	0.0357	0.0357	0.0445	0.0445	0.0172	0.0172	0.0172	0.0172	0.0179	0.0179
5.00	0.10	0.0532	0.0532	0.0532	0.0532	0.0639	0.0639	0.0283	0.0283	0.0282	0.0282	0.0375	0.0375	0.0201	0.0201	0.0201	0.0201	0.0221	0.0221
	0.30	0.0529	0.0529	0.0530	0.0530	0.0636	0.0636	0.0283	0.0283	0.0282	0.0282	0.0375	0.0375	0.0202	0.0202	0.0202	0.0202	0.0223	0.0223
	0.50	0.0529	0.0529	0.0530	0.0530	0.0636	0.0636	0.0282	0.0282	0.0282	0.0282	0.0375	0.0375	0.0203	0.0203	0.0203	0.0203	0.0223	0.0223
10.0	0.10	0.0532	0.0532	0.0532	0.0532	0.0639	0.0639	0.0281	0.0281	0.0281	0.0281	0.0374	0.0374	0.0201	0.0201	0.0201	0.0201	0.0221	0.0221
	0.30	0.0529	0.0529	0.0529	0.0529	0.0636	0.0636	0.0281	0.0281	0.0281	0.0281	0.0374	0.0374	0.0202	0.0202	0.0202	0.0202	0.0223	0.0223
	0.50	0.0528	0.0528	0.0528	0.0528	0.0635	0.0635	0.0280	0.0280	0.0280	0.0280	0.0373	0.0373	0.0203	0.0203	0.0203	0.0203	0.0224	0.0224

Table 3 Non-dimensional critical loads of fan-type bridge subjected to full lane load with H-type pylon

I_p/I_b	H/L	L_1/L																	
		0.4						0.6						0.8					
		1st Mode	2nd Mode	3rd Mode	4th Mode	5th Mode	6th Mode	1st Mode	2nd Mode	3rd Mode	4th Mode	5th Mode	6th Mode	1st Mode	2nd Mode	3rd Mode	4th Mode	5th Mode	6th Mode
0.10	0.10	0.0433	0.0433	0.0433	0.0433	0.0515	0.0515	0.0261	0.0261	0.0261	0.0261	0.0337	0.0337	0.0134	0.0134	0.0134	0.0134	0.0140	0.0140
	0.30	0.0433	0.0433	0.0433	0.0433	0.0515	0.0515	0.0261	0.0261	0.0262	0.0262	0.0337	0.0337	0.0134	0.0134	0.0134	0.0134	0.0140	0.0140
	0.50	0.0434	0.0434	0.0434	0.0434	0.0515	0.0515	0.0262	0.0262	0.0262	0.0262	0.0337	0.0337	0.0135	0.0135	0.0135	0.0135	0.0140	0.0140
5.00	0.10	0.0406	0.0406	0.0406	0.0406	0.0487	0.0487	0.0215	0.0215	0.0216	0.0216	0.0286	0.0286	0.0153	0.0153	0.0154	0.0154	0.0169	0.0169
	0.30	0.0403	0.0403	0.0403	0.0403	0.0484	0.0484	0.0214	0.0214	0.0214	0.0214	0.0285	0.0285	0.0154	0.0154	0.0154	0.0154	0.0170	0.0170
	0.50	0.0403	0.0403	0.0403	0.0403	0.0484	0.0484	0.0213	0.0213	0.0213	0.0213	0.0284	0.0284	0.0155	0.0155	0.0156	0.0156	0.0171	0.0171
10.0	0.10	0.0405	0.0405	0.0405	0.0405	0.0487	0.0487	0.0214	0.0214	0.0214	0.0214	0.0285	0.0285	0.0153	0.0153	0.0153	0.0153	0.0169	0.0169
	0.30	0.0403	0.0403	0.0403	0.0403	0.0484	0.0484	0.0212	0.0212	0.0212	0.0212	0.0283	0.0283	0.0154	0.0154	0.0154	0.0154	0.0170	0.0170
	0.50	0.0402	0.0402	0.0402	0.0402	0.0483	0.0483	0.0211	0.0211	0.0212	0.0212	0.0282	0.0282	0.0155	0.0155	0.0156	0.0156	0.0171	0.0171

stay cables, as well as between the bridge deck and the pylons. These angles are responsible for different axial force at different locations on the bridge deck and pylons. These axial forces cause geometric nonlinearity, especially for flexible pylon.

Fig. 2 represents the comparison of the first 6 buckling modes of fan-type and harp-type bridges with the same designed parameters: I_p/I_b=1.0, H/L=0.1, and L_1/L=0.6. The figures show that the fundamental modes of these bridges with a set of given design parameters are similar to each other; they are anti-symmetric torsion mode; however, the fan-type bridge has about 24% of critical load

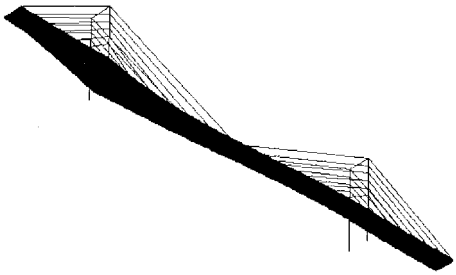

Fig. 2(a)-1 The 1st buckling mode shape of harp-type bridge with H-type of pylon and parameters: I_p/I_b=1.0, H/L=0.1, L_1/L=0.6, b/a=1.0

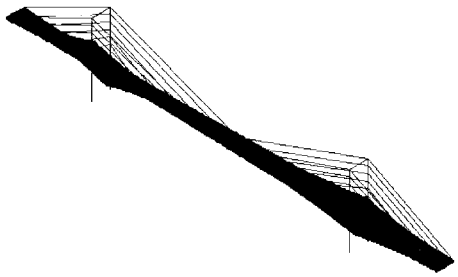

Fig. 2(a)-4 The 4th buckling mode shape of harp-type bridge with H-type of pylon and parameters: I_p/I_b=1.0, H/L=0.1, L_1/L=0.6, b/a=1.0

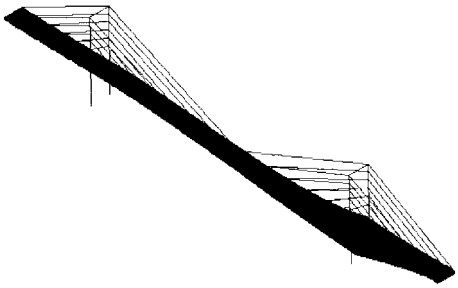

Fig. 2(a)-2 The 2nd buckling mode shape of harp-type bridge with H-type of pylon and parameters: I_p/I_b=1.0, H/L=0.1, L_1/L=0.6, b/a=1.0

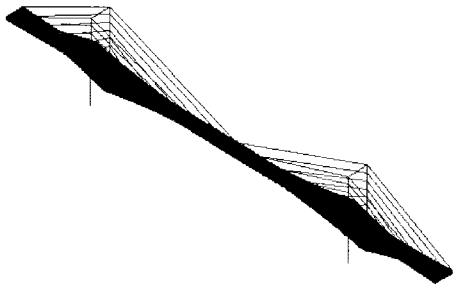

Fig. 2(a)-5 The 5th buckling mode shape of harp-type bridge with H-type of pylon and parameters: I_p/I_b=1.0, H/L=0.1, L_1/L=0.6, b/a=1.0

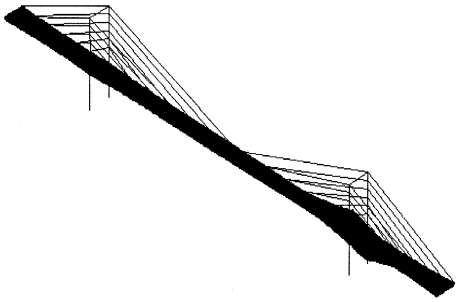

Fig. 2(a)-3 The 3rd buckling mode shape of harp-type bridge with H-type of pylon and parameters: I_p/I_b=1.0, H/L=0.1, L_1/L=0.6, b/a=1.0

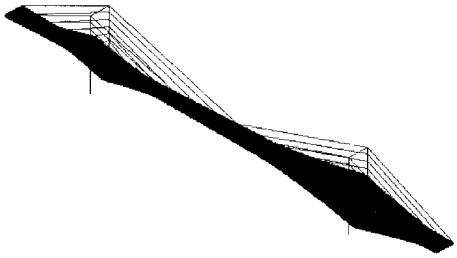

Fig. 2(a)-6 The 6th buckling mode shape of harp-type bridge with H-type of pylon and parameters: I_p/I_b=1.0, H/L=0.1, L_1/L=0.6, b/a=1.0

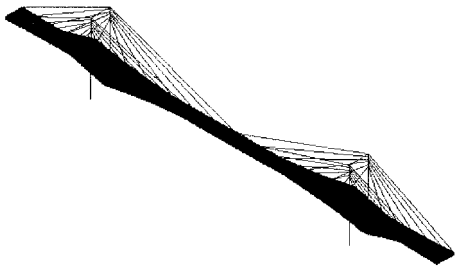

Fig. 2(b)-1 The 1st buckling mode shape of fan-type bridge with H-type of pylon and parameters: I_p/I_b=1.0, H/L=0.1, L_1/L=0.6, b/a=1.0

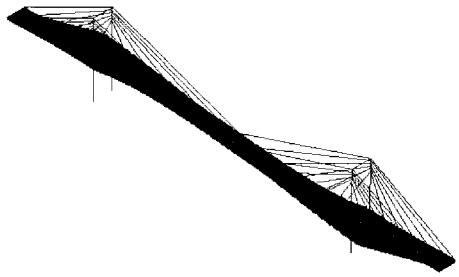

Fig. 2(b)-4 The 4th buckling mode shape of fan-type bridge with H-type of pylon and parameters: I_p/I_b=1.0, H/L=0.1, L_1/L=0.6, b/a=1.0

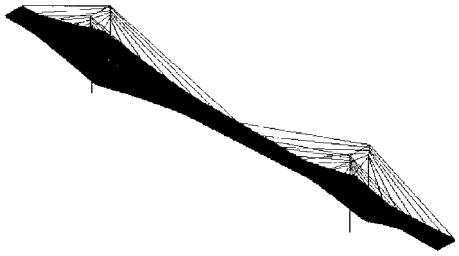

Fig. 2(b)-2 The 2nd buckling mode shape of fan-type bridge with H-type of pylon and parameters: I_p/I_b=1.0, H/L=0.1, L_1/L=0.6, b/a=1.0

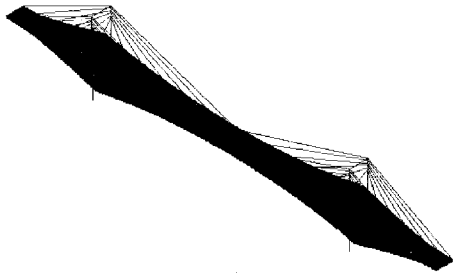

Fig. 2(b)-5 The 5th buckling mode shape of fan-type bridge with H-type of pylon and parameters: I_p/I_b=1.0, H/L=0.1, L_1/L=0.6, b/a=1.0

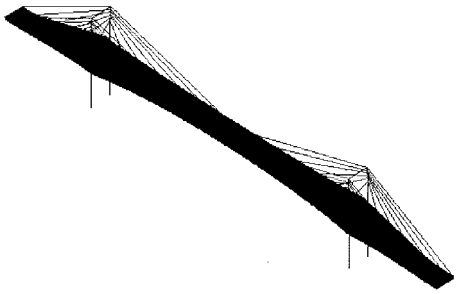

Fig. 2(b)-3 The 3rd buckling mode shape of fan-type bridge with H-type of pylon and parameters: I_p/I_b=1.0, H/L=0.1, L_1/L=0.6, b/a=1.0

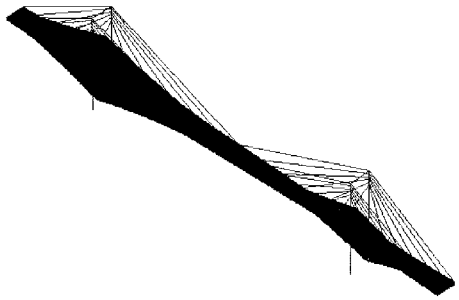

Fig. 2(b)-6 The 6th buckling mode shape of fan-type bridge with H-type of pylon and parameters: I_p/I_b=1.0, H/L=0.1, L_1/L=0.6, b/a=1.0

lower than that of harp-type bridge.

Fig. 3 presents the relationships between the critical load and the designed parameter L_1/L for H/L=0.1, and various I_p/I_b ranging from 0.1 to 10.0 in which the bridge supported by H-type of pylon with fan-type cable arrangement is subjected to full lane load.

Fig. 3 indicates that the critical load decreases as I_p/I_b increases with a few exceptions. This type of cable-stayed bridge with smaller I_p/I_b and L has higher critical load due to flexible pylon and stiff bridge deck; it has stronger interaction among the substructures. When the ratio I_p/I_b reaches

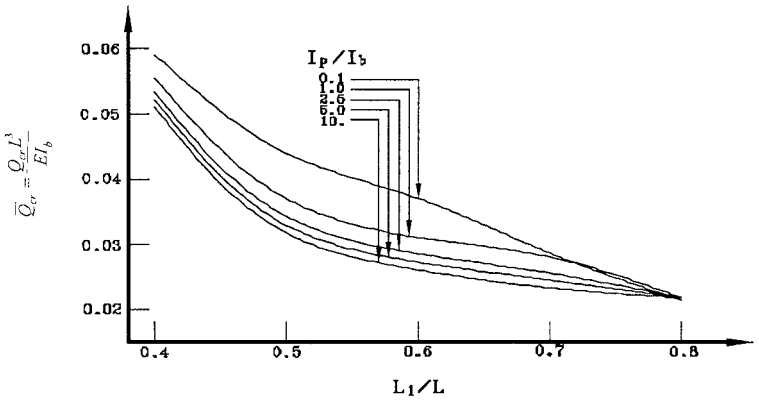

Fig. 3 Non-dimensional critical loads versus design parameter L_1/L for various I_p/I_b with H-type of pylon and fan-type of cable arrangement under full lane load

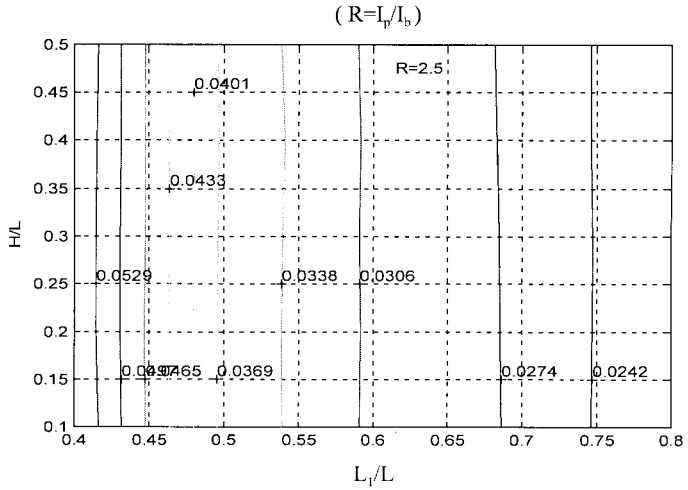

Fig. 4 Contour plot of critical loads with H-type of pylon and harp-type of cable arrangement under full lane load

1.0, the critical load is no more significantly decreased.

Fig. 4 presents the contours of critical loads in terms of designed parameters L_1/L versus H/L. With a constant total span length, a cable-stayed bridge has lower critical load when its main span length increases. Fig. 4 shows that the critical load decreases when the L_1/L increases. If L_1/L is less than 0.6, its effect on buckling analysis is significant for the further increment. If L_1/L is greater than 0.6, the critical load decreases but the changes are not significant compared to those of the bridges with the small L_1/L. Meanwhile, Fig. 4 shows that the designed parameter H/L has only a slight effect on buckling analysis of this type of bridge. In other words, the effect of the height of the pylon above the bridge deck is not significant on buckling analysis of this type of cable-stayed bridge.

Fig. 5 represents the non-dimensional critical loads versus the designed parameter b/a for various L_1/L ranging from 0.4 to 0.8 with 0.1 apart. In Fig. 5, the bridge is subjected to full lane load with

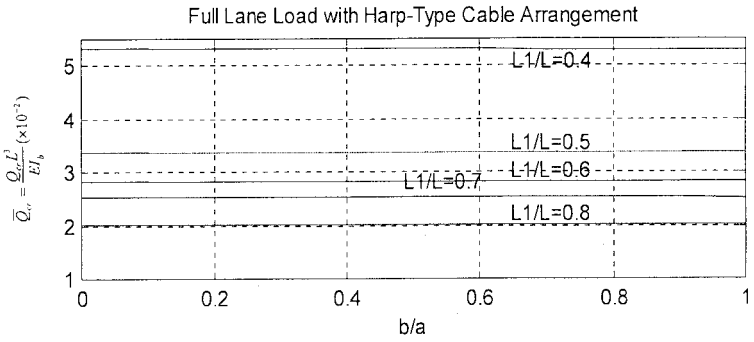

Fig. 5 Non-dimensional critical load versus b/a for various L_1/L

designed parameter b/a ranging form 0 to 1.0. It shows that the shapes of pylon have no effect on buckling analysis of this type of bridge.

With the horizontal and vertical components of the cable reaction acting on the bridge deck and

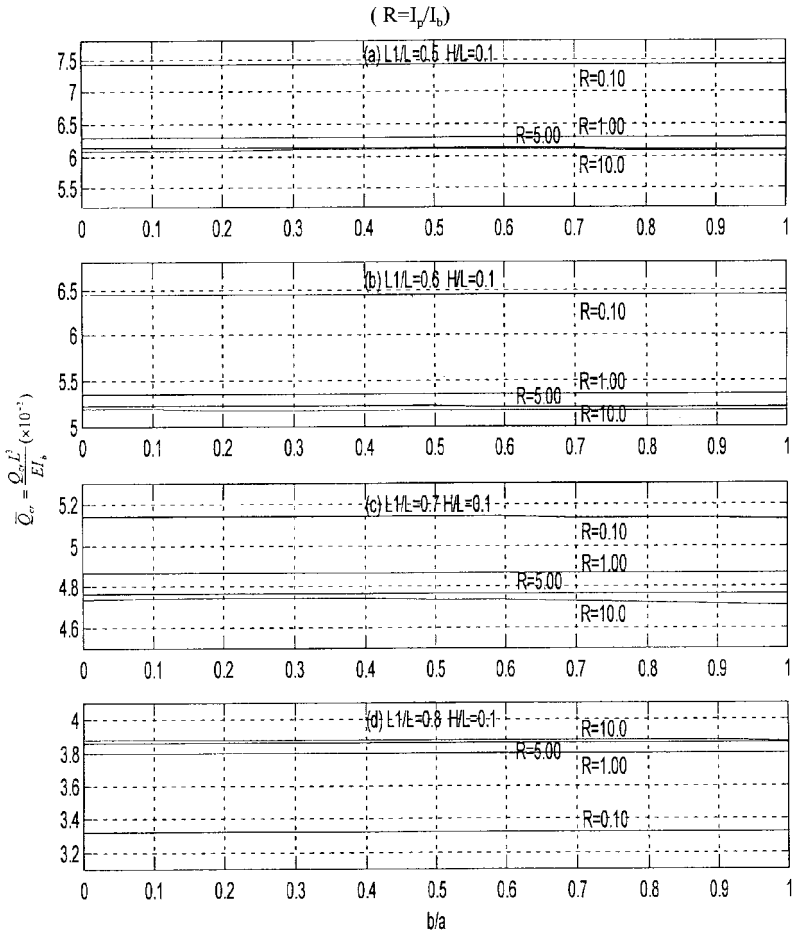

Fig. 6 Non-dimensional critical load versus b/a for various I_p/I_b

pylons, respectively, the effects of I_p/I_b on buckling analysis must be investigated (Vlahinos *et al.* 1992 and Wang 1999c). Fig. 6 plots the non-dimensional critical loads versus various types of pylon for designed parameters L_1/L ranging form 0.5 to 0.8 and I_p/I_b ranging from 0.1 to 10.0. In Fig. 6, the ratio H/L remains constant 0.2. As the ratio I_p/I_b increases, the critical loads decrease for all cases. If the ratio of I_p/I_b is greater than 1.0, the critical loads decrease slightly. Fig. 6 indicates that the critical loads decrease as the ratio I_p/I_b increases if L_1/L is equal to or less than 0.7 because the stiffness of pylon reduces the interaction among the substructures such as the pylon, bridge deck, and stayed cables. The critical loads are almost the same for all bridges supported by different types of pylon. If L_1/L is equal to 0.8, the pylon is subjected to strong axial force transferred from the stayed cables, which causes the pylon buckled. The numerical results also show that if H/L equals to 0.1, the characteristics of critical load are similar to those where H/L=0.2. In other words, H/L has no significant effect on buckling analysis for this type of bridge.

Fig. 7 represents the non-dimensional critical loads versus L_1/L for different combinations of cable arrangement and load condition. In Fig. 7, the bridges are supported by H-type of pylon with a variety of designed parameters H/L and I_p/I_b. The bridges subjected to full lane load with fan-type cable arrangement always have the lowest critical loads. Bridges with harp-type cable arrangement under half-diagonal load condition have the highest critical loads. Fig. 7 also indicates that the critical loads of the bridge with fan-type cable arrangement under the half load condition are almost the same as those of the bridge with fan-type cable arrangement under half-diagonal load condition,

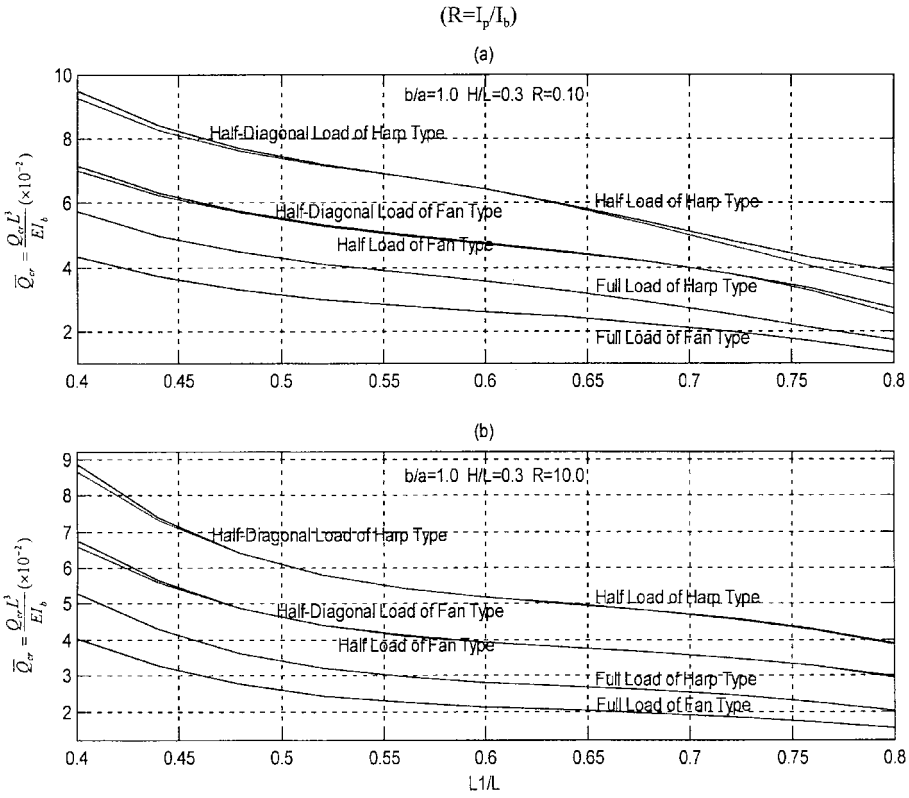

Fig. 7 Non-dimensional critical loads versus L_1/L for different cable arrangements and load conditions

for all L_1/L. When the ratio I_p/I_b reaches 1.0, the critical load decreases more rapidly than that of the bridges having the ratio I_p/I_b less than 10.0.

5. Concluding remarks

1. Because of the horizontal component of the cable reactions acting on the bridge deck and the vertical component of the cable reactions acting on the pylon, the cable-stayed bridge with fan-type cable arrangement always has lower critical load compared to that of the bridge with harp-type cable arrangement.
2. Because of the lack of interactions among the substructures such as the bridge deck, stayed cables, and pylons, the bridge supported by stronger pylons has the lower critical load.
3. With a constant total span length, the longer the main span, the lower critical loads it has for this type of bridge.
4. Bridges subjected to the lane full load conditions always have the lowest critical load especially for fan-type bridges.
5. The shapes of pylon varying from A-type to H-type have no significant effect on buckling analysis of these types of cable-stayed bridges because no torsion of fan was considered.

References

Adeli, H. and Zhang, J. (1995), "Fully nonlinear analysis of composite girder cable-stayed bridges", *Computers and Structures*, **54**(2), 267-277.

Agrawal, T.P. (1997), "Cable-stayed bridges parametric study", *Journal of Bridge Engineering*, ASCE, **2**(2), 61-67.

Agrawal, T.P. (1998), "Closure of cable-stayed bridges-parametric study", *Journal of Bridge Engineering*, ASCE, **3**(3), 150-150.

ASCE (1988), "Bibliography and data on cable-stayed bridges", *ASCE Committee on Long-Span Steel Bridges, J. Struct. Div.*, ASCE, **103**(ST10), October.

ASCE Committee on Cable-Stayed Bridges (1992), "Guidelines for the design of cable-stayed bridges", ASCE.

Bathe, K.-J. (1982), "Finite element procedures in engineering analysis", Prentice-Hill, Inc.

Capra, A. and Leveille, A. (1998), "Vasco da Gama Bridge, Portugal", *Structural Engineering International*, IABSE, **8**(4), 261-262.

Cluley, N.C. and Shepherd, R. (1996), "Analysis of concrete cable-stayed bridges for creep, shrinkage and relaxation effects", *Computers & Structures*, **58**(2), 337-350.

Committee on General Structures Subcommittee on Bridge Aesthetics (1991), "Bridge aesthetics around the world", Transportation Research Board, National Research Council, Washington, D.C.

Ermopoulos, J.CH., Vlahinos, A.S., and Wang, Yang-Cheng (1992), "Stability analysis of cable-stayed bridges", *Computers & Structures*, **44**(5), 1083-1089.

Freeman, R.A. (1994), "Innovative cable erection system for cable-stayed bridges", *Proceedings of the Institution of Civil Engineers Structures and Buildings*, 243-250.

Gardner-Morse, M.G. and Huston, D.R. (1993), "Modal identification of cable-stayed pedestrian bridge", *Journal of Structural Engineering*, ASCE, **119**(11), 3384-3404.

Hwa, C.-H. and Wang, Yang-Cheng (1996), "Three-dimensional modeling of a cable-stayed bridge for dynamic analysis", *Proceedings of International Modal Analysis, National Science Council (Taiwan)*, **II**, 1565-1571.

Ito, M. (1998), "Wind effects improve tower shape", *Structural Engineering International*, IABSE, **8**(4), 256-257.

Leu, Y.-C. and Wang, Yang-Cheng (1996), "Stability analysis of cable-stayed bridges with cable safety", *The*

Third Military Academy Symposium on Fundamental Science, Taiwan, 161-166.
Modjeski and Masters (1983), "Structural drawings of quincy bayview bridge", Modjeski and Masters Consulting Engineers, Harrisburg, Pennsylvania.
Oh, I.L. *et al.* (1998), "Fabrication of the box girder of Kao-Pin Hsi cable-stayed bridges", *Proceedings of the 4th National Conference on Structural Engineering*, National Science Council (Taiwan), **3/3**, 1479-1486.
Ren, W.-X. (1999), "Ultimate behavior of long-span cable-stayed bridges", *Journal of Bridge Engineering*, ASCE, **4**(1), 30-37.
Ren, W.-X. and Obata, M. (1999), "Elastic-plastic seismic behavior of long span cable-stayed bridges", *Journal of Bridge Engineering*, ASCE, **4**(3), 194-203.
Simoes, L.M.C. and Negrao, J.H.O. (1994), "Sizing and geometry optimization of cable-stayed bridges", *Computers & Structures*, **53**(2), 309-321.
Tang, M.-C. (1971), "Analysis of cable-stayed bridges girder bridges", *Journal of the Structural Division*, ASCE, **97**(ST5), 1481-1496.
Vlahinos, A.S. and Wang, Yang-Cheng (1994), "Nonlinear dynamic behavior of cable-stayed bridges", *Proceedings of the 12th International Modal Analysis Conference*, **II**, 1335-1341.
Vlahinos, A.S., Ermopoulos, J. CH. and Wang, Yang-Cheng (1993), "Buckling analysis of steel arch bridges", *Journal of Constructional Steel Research*, **26**, 59-71.
Vlahinos, A.S. and Wang, Yang-Cheng (1993), "Effect of supporting conditions on the critical loads of cable-stayed bridges", *the Proceedings of the Twenty-Third Midwestern Mechanics Conference*, University of Nebraska, 190-192.
Wang, Yang-Cheng, Vlahinos, A.S. and Shu, H.-S. (1997), "Optimization of cable preloading on cable-stayed bridges", *Proceedings of the International Society for Optical Engineering*, 248-259.
Wang, Yang-Cheng and Ermopoulos, J. (1997), "Optimum design of cable-stayed bridges using 3D buckling analysis", *Proceedings of the International Colloquium on Computation of Shell and Spatial Structures*, 289-294.
Wang, Yang-Cheng, Chen, P.L. and Shu, H.-S. (1998), "Three-dimensional modeling of Kao-Pin Shi cable-stayed bridge for dynamic analysis", *Proceedings of the 4th National Conference on Structural Engineering*, National Science Council (Taiwan), **3/3**, 1583-1589.
Wang, Yang-Cheng (1999a), "Characteristics of cable stiffness on a cable-stayed bridge", *Structural Engineering and Mechanics*, **8**(1), 27-38.
Wang, Yang-Cheng (1999b), "Kao-Pin Hsi cable-stayed bridge, Taiwan", *Structural Engineering International*, IABSE, **9**(2), 94-95.
Wang, Yang-Cheng (1999c), "Number of cable effects on buckling analysis of cable-stayed bridges", *Journal of Bridge Engineering*, ASCE, **4**(4), 242-248.
Walton, J.M. (1996), "Developments in steel cables", *Journal of Constructional Steel Research*, **39**(1), 3-29.
Wilson, J.C. and Gravelle W. (1991), "Modelling of a cable-stayed bridge for dynamic analysis", *Earthquake Engineering and Structural Dynamics*, **20**, 707-721.
Xanthakos, P.P. (1994), *Theory and Design of Bridges*, John Wiley & Sons, Inc. New York, N.Y.
Xi, Y. and Kuang, J.S. (1999), "Ultimate load capacity of cable-stayed bridges", *Journal of Bridge Engineering*, ASCE, **4**(1), 14-22.
Yang, F. and Fonder, G.A. (1998), "Dynamic response of cable-stayed bridges under moving loads", *Journal of Engineering Mechanics*, ASCE, **124**(7), 741-747.

Notation

a : length of the lower strut
b : distance between the tops of the two towers
E : modulus of elasticity
EI_b : rigidity of the bridge deck
H : height of the pylon from bridge deck to the top of pylon
H_1 : height of the pylon from pier top to bridge deck

L : total span length of the cable-stayed bridge
L_1 : main span length of the cable-stayed bridge
I_b : moment of inertia of the bridge deck
I_p : moment of inertia of the pylon
Q_{cr} : critical load obtained by finite element methods
$\overline{Q}_{cr}$: non-dimensional critical load
ν : Poisson's ratio